Mon. Not. R. astr. Soc. (1980) **193**, 683–706

Models of the cosmological evolution of extragalactic radio sources – I. The 408-MHz source count

J. V. Wall*, T. J. Pearson† and M. S. Longair‡ *Mullard Radio Astronomy Observatory, Cavendish Laboratory, Madingley Road, Cambridge CB3 0HE*

Received 1980 March 27

Summary. A simple numerical procedure for analysing the counts of extragalactic radio sources is described. The scheme makes efficient use of the extensive data base which is now available for studying the spatial distribution of radio sources.

The method is first applied to data at 408 MHz. We show that, if proper statistical testing is incorporated, the technique provides strong support for the qualitative conclusions of previous analyses: the comoving density of the more powerful radio sources with extended structure is now less than at earlier epochs by a factor of $\gtrsim 10^3$. However, several evolution models proposed earlier are quantitatively unsatisfactory, and new models are derived which adequately describe the current data. These new models make contrasting predictions about redshift distributions amongst the faint radio sources ($S_{408} \geqslant 10$ mJy), and identification data at such levels can therefore provide powerful constraints upon the models.

Our results are compared with results from recent investigations of the spatial distribution of steep-spectrum radio sources.

1 Introduction

The past few years have seen a dramatic increase in the quantity and quality of the data on which to base statistical studies of the spatial distribution of extragalactic radio sources (see, e.g. Jauncey 1977). At frequencies at 1415 MHz and lower, the source counts or $N(S)$ relations have been determined to flux densities corresponding to surface densities of 10^5 sources sr^{-1}. For the stronger sources found at these frequencies, continued programmes with the largest optical telescopes have increased the optical identification content to completeness levels exceeding 90 per cent in some samples. At the higher frequencies of 2700 and 5000 MHz, surveys now covering most of the sky have revealed the extent of the 'flat-spectrum' or 'centimetre-excess' source population; identification programmes have shown that the majority of such sources have QSOs as their optical counterparts. Statistical

*Present address: Royal Greenwich Observatory, Herstmonceux Castle, Hailsham, Sussex.
†Present address: Owens Valley Radio Observatory, California Institute of Technology, Pasadena, California 91125, U.S.A.
‡Present address: Royal Observatory, Blackford Hill, Edinburgh, Scotland.

methods have been used to extend the high-frequency $N(S)$ relations to source densities comparable with those of the low-frequency counts.

The increased precision with which the overall source counts are now known and improved determinations of the luminosity distributions have prompted us to investigate what new bounds can be set to the evolution of the radio source population as a function of cosmological epoch or redshift. In particular, we want to know how much can be added to the early conclusions which were drawn from the source counts, namely (i) that the counts (of necessity at frequencies of $\leqslant 408$ MHz) indicated strong cosmological evolution for the steep-spectrum sources, the comoving densities of powerful sources exceeding present-day densities by factors $\gtrsim 10^3$ at redshifts of 2 or 3, and (ii) that the evolution is confined to powerful sources, those in the 'upper end' of the luminosity function.

These conclusions were supported by applications of the luminosity–volume ($V/V_{\max}$) test to samples of QSOs from low-frequency surveys (e.g. Schmidt 1968; Lynds & Wills 1972). This test provides the more direct demonstration of the change of density with cosmic epoch, although the results are not independent of the results of source-count analysis (Longair & Scheuer 1970) – indeed they cannot be so, since the same objects are involved. The $V/V_{\max}$ test is necessarily confined to limited samples of objects with measured redshifts which span a small range in flux density. The count data now span flux-density ranges of 10^4, based on several thousand radio sources and analyses in which radio and optical data on individual objects are systematically incorporated can yield significant additional information on the spatial distribution of all source types or populations which constitute these counts.

The present paper (the first of two) is the first step towards such a systematic interpretation of the modern data. The emphasis is threefold: (1) the description of a simple numerical technique which makes efficient use of the data, (2) the comparison of models with observations using appropriate statistical procedures, and (3) the determination of which new observations are most important in defining the cosmological evolution with greater precision.

The scheme and some of these results were summarized at *IAU Symposium No. 74* (Wall, Pearson & Longair 1977). The present paper describes the procedure in greater detail and incorporates new results which have become available since that time. It concentrates on the interpretation of the source counts at low frequencies, whilst the companion paper (Paper II) deals with the problems of the high-frequency source counts with the emphasis upon the counts at 2.7 GHz.

Section 2 presents the method and contrasts it with earlier techniques. The 408-MHz data to which the method is applied in this paper are discussed in Section 3. In Section 4 some unsatisfactory models which have been widely used in the literature are examined critically, together with two new models which meet with greater success. The discussion of Section 5 compares the results of the present scheme with results derived by other authors.

2 The Scheme

We want to know the generalized radio luminosity function

p (P, z, *radio source type*)

which describes the comoving space density of radio sources as a function of radio power P, redshift z (i.e. epoch – we assume that redshifts are cosmological distance indicators), and *radio source type*. This last parameter includes the other information about the sources: spectrum, structure, optical properties etc. We shall regard *radio source type* as a parameter distinguishing a number of discrete populations of radio source whose evolution

may be considered independently if there is adequate observational evidence to justify such a refinement. The generalized luminosity function describes the cosmic history of the various populations of radio sources, from the objects of highest power – radio galaxies and QSOs with extended structures and steep radio spectra, and the QSOs with compact radio structures and 'flat' spectra – through to the low-power objects identified with nearby galaxies and which exhibit a wide variety of radio spectra and structures.

A description of the usual procedure for analysing a source count highlights the difficulties and lays down the essential theory:

(1) Assume that the source count at frequency ν is composed of a *single* source population, for which one luminosity function $\rho(P, z)$ is applicable, and for which a single spectral index is a good approximation. As all the sources have the same spectrum, the radio power P can be taken as the monochromatic luminosity P_ν in the rest frame of the source.

(2) Factorize ρ in the following way:

$$\rho\,(P, z) = F(P_\nu, z)\,\rho_0\,(P_\nu), \tag{1}$$

where F is the *evolution function* and ρ_0 is the *local lumonisity function.* There is no loss of generality in this factorization, in that F describes the change in ρ with epoch, and it can represent so-called 'density' evolution or 'luminosity' evolution (if these are distinguishable), or a mixture of both.

(3) Assume a world model. This provides the relation between flux density and luminosity

$$S_\nu = P_\nu / D^2 (1+z)^{1+\alpha}, \tag{2}$$

and the relation between comoving volume and redshift

$$dV(z) = 4\pi D^2 dr, \tag{3}$$

where α is the spectral index defined in the sense $S \propto \nu^{-\alpha}$ and D is the 'effective distance' (equivalent to the term $\sin Ar/A$ in the notation of Scheuer 1975; see also Longair 1978). In Friedmann world models ($\Lambda = 0$), D is a function of the cosmological parameters H_0, the Hubble constant, and Ω, the density parameter, according to the relation

$$D = \frac{2c}{H_0\,\Omega^2\,(1+z)}\,[\Omega z - (\Omega - 2)\,\{(\Omega z + 1)^{1/2} - 1\}], \tag{4}$$

and dr is the element of comoving coordinate distance $dr = cdz/H_0\,(1+z)\,(\Omega z + 1)^{1/2}$.

(4) Make an estimate of the local luminosity function $\rho_0\,(P_\nu)$. The problem with this step is that the crucial part of the function is at high radio luminosities and can only be derived from very distant sources. At these large distances, the effects of cosmological evolution cannot be neglected. Thus, as has been known for a long time, the local luminosity function cannot be determined independent of the answer which is the object of the exercise.

(5) Populate the P–z or evolution plane with a model for the evolution function $F(P_\nu, z)$. In our numerical scheme, the plane is divided into strips ΔP in width covering the observed range in luminosity of the radio sources, and strips Δz in width from $z = 0$ to $z = \infty$, or (in practice) out to a z at which the most powerful source will be too faint to contribute to the faintest flux-density bin of the count under analysis.

(6) Compute the source count; each bin $(\Delta P_{\nu i}, \Delta z_j)$ contributes to the count

$$n_{ij} = \frac{1}{4\pi}\,F(P_i, z_j)\,\rho_0(P_i)\,\Delta V(z_j) \text{ sources sr}^{-1} \tag{5}$$

of flux density S_i, where S_i is obtained from equation (2) for (P_i, z_j), and $\Delta V(z_j)$ is the volume in the redshift shell Δz_j (equation 3). The source-count may be written in integral form as follows:

$$N(\geqslant S) = \int_0^\infty dP \int_0^{z(S)} \rho_0(P)\, F(P, z)\, dV(z). \tag{6}$$

In the numerical scheme, the integral is replaced by a sum over all values of i and j such that

$$S \leqslant \frac{P_i}{D^2(z_j)\,(1+z_j)^{1+\alpha}}.$$

Compare the count with the observed count.

(7) Calculate the relevant *luminosity distribution(s),* the frequency distribution of radio powers for a complete sample of sources with flux density $\geqslant S_0$. Considering the evolution plane again, the distribution is

$$n(P_i) = \sum_{j=1}^{j(S_0)} n_{ij}, \tag{7}$$

where $j(S_0)$ is the index at which $z = z(S_0)$, the solution of (2) for the redshift at which a source of P_i has a flux density of S_0. Formally,

$$n(P)dP = dP \int_0^{z(S_0)} F(P, z)\, \rho_0(P)\, dV(z). \tag{8}$$

Compare this luminosity distribution with that obtained from the identification data.

(8) If comparisons (6) and (7) are unsatisfactory, return to steps (4) and (5); adjust ρ_0 and/or F; try again.

The difficulty with this procedure is how to make efficient adjustment to satisfy both the counts and the optical data (luminosity distributions). Equation (6) suggests a way of improving the procedure. If a *complete* luminosity distribution is available, constructed from a large enough number of sources to guarantee statistical accuracy at all luminosities of interest, then the assumption of an evolution function leads to a unique solution for the local luminosity function:

$$\rho_0(P)dP = \frac{n(P)dP}{\int_0^{z(P, S_0)} F dV} = \frac{n_i\, \Delta P_i}{\sum_{j=1}^{j(P_i, S_0)} F(P_i, z_j)\, \Delta V(z_j)}. \tag{9}$$

The essence of our scheme, therefore, is to start with a luminosity distribution and an assumed evolution function, from which we generate first ρ_0 (equation 9), and then the source count (equation 5). The advantage of this procedure is that, at the present time, the only luminosity distributions which are almost completely defined are those at the highest flux densities for which there have been extensive surveys for optical identifications and redshifts. At lower flux densities, the optical data are much less complete and consequently do not provide a basis for defining the overall distribution. The present procedure therefore guarantees that whatever function $F(P, z)$ is adopted, we will always reproduce correctly the luminosity distribution where it is best determined. Our goal is then to find evolution functions which will provide a satisfactory fit to the source counts and to the rather incomplete luminosity distributions at lower flux densities.

The approach may be generalized to the analysis of counts in which two or more populations are present; complete luminosity distributions for each population are required. Furthermore it may be generalized to the situation when complete luminosity distributions become available at more than one flux-density. A solution for ρ_0 may be obtained from a weighted combination of these distributions:

$$\rho_0(P)dP = \frac{1}{\Sigma w_k(P)} \sum \frac{w_k(P)n_k(P)dP}{\int_0^{z_k(S_{0k})} F(P, z)\, dV(z)}, \tag{10}$$

where w_k are appropriately chosen weights. However, before accepting this estimate of ρ_0, the luminosity distribution produced at each S_{0k} should be compared statistically with that observed. It may be that such a comparison rules out the assumed F before $N(S)$ need be computed.

The details of our scheme are shown in Fig. 1. The requisite input *data* are shown on the left. The input *guesses*, shown to the right, consist of the evolution model (the object of the exercise), and a world model. We have used two Friedmann models ($\Lambda = 0$), namely the Milne model ($\Omega = 0, q_0 = 0$) for which

$$D = \frac{c}{H_0}\left\{\frac{1}{2}\left[(1+z) - \frac{1}{(1+z)}\right]\right\} \tag{11}$$

and the Einstein – de Sitter model ($\Omega = 1, q_0 = 0.5$) for which

$$D = \frac{c}{H_0}\left\{2\left[1 - \frac{1}{\sqrt{1+z}}\right]\right\}. \tag{12}$$

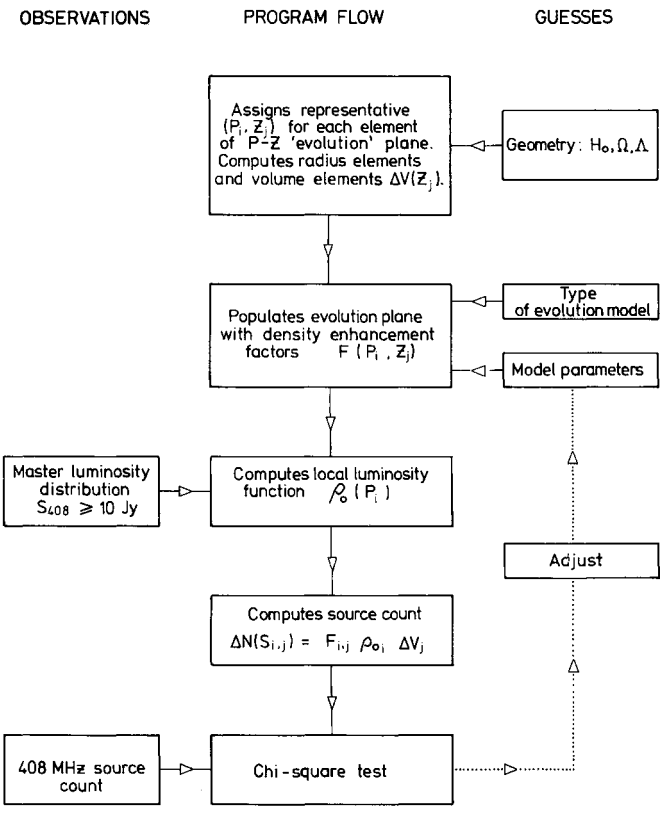

Figure 1. Flow diagram for source-count computation; see Section 2.

We adopted $H_0 = 50\,\mathrm{km\,s^{-1}\,Mpc^{-1}}$ – a constant which does not enter source-count calculations explicitly, but constituents and by-products of the sums such as local luminosity functions and luminosity distributions require its specification.

Table 1. The 408-MHz source count.

S_{408} (Jy)	Area surveyed (sr)	Number found	ΔN ($\mathrm{sr^{-1}}$)	Reference
∞				
	10.1	14	1.4	All-sky catalogue (Robertson 1973)
40.0				
	10.1	14	1.4	
28.3				
	10.1	20	2.0	
20.0				
	10.1	28	2.8	
14.1				
	10.1	84	8.3	
10.0				
	1.5	32	21	Bologna B2 survey (Colla *et al.* 1973)
6.329				
	1.2	23	19	
5.038				
	1.6	42	26	
4.010				
	1.3	64	48	
3.191				
	1.3	81	63	
2.541				
	1.5	153	99	
2.021				
	1.5	237	154	
1.609				
	1.4	264	195	
1.281				
	1.3	379	292	
1.020				
	0.72	274	381	
0.811				
	0.54	279	518	
0.646				
	0.32	239	758	
0.514				
	0.25	220	889	
0.409				
	0.15	167	1100	
0.325				5C2 + 5C5 surveys (Pooley & Kenderine 1968; Pearson 1975)
0.218				
	0.00746	45	6060	
0.109				
	0.00747	65	8700	
0.063				
	0.00507	92	18140	
0.032				
	0.00282	35	12400	
0.021				
	0.00073	22	29970	
0.012				

In the scheme, we choose analytic functions $F(P, z)$ of somewhat general form which involve a small number of undetermined parameters. For a given set of these parameters, the programme works out the local luminosity function $\rho_0(P_i)$ and the source counts $\Delta N(S_i)$. The predicted counts are then converted into the numbers of sources expected in differential flux density intervals *in the actual radio surveys themselves*. In the way, the numbers of sources observed in the sky are compared directly with the models (see Table 1). An appropriate measure of the adequacy of the model in accounting for the source counts is provided by a χ^2-test. If the χ^2-test indicates a poor fit, a new set of parameters is chosen and the procedure repeated. In practice, what is done is to make a search throughout the whole of the relevant region of parameter space, and the minimum value of χ^2 found indicates how well models of different functional forms can explain the source counts. A large computer is required to perform this procedure rapidly and the Cambridge University IBM 370 was used for these experiments. The computations were made by splitting up the P–z plane into 100 equal logarithmic intervals between $\log (P_{408}/\mathrm{W\,Hz^{-1}\,sr^{-1}}) = 20.0$ and 30.0 in radio luminosity and 100 such intervals in redshift between $z = 0.01$ and 100.

In our procedure, we use a master luminosity distribution $n(P, S)$ defined at 10 Jy at 408 MHz which is described in the next section. A limitation of our testing procedure is that we do not take account of the statistical uncertainties in this distribution in making the comparison of the predicted and observed counts. There is regretably no simple way of estimating how much this uncertainty effects the values of χ^2. This is because different models give different weights to different portions of the input luminosity distribution. Ideally, we could estimate the errors by running Monte Carlo simulations of each model tested but this would be prohibitively expensive in computing time. We expect this uncertainty to contribute only a small effect, because the precise shape of the luminosity function is not what makes model-fitting difficult. As will become apparent, the difficulty in finding satisfactory models for the overall counts lies in the forms of $F(P, z)$ rather than in $n(P, S)$.

3 Analysis of the 408-MHz source count; the data

The incentive for this approach came from our initial examination of current data at 408 MHz. First, $\gtrsim 90$ per cent of the sources catalogued above 1 Jy at this frequency are of the 'steep-spectrum' type. For the present exercise, we therefore made the simplifying assumption that *all* sources of the 408-MHz count rate are of this type, and we adopted a single spectral index of $\alpha = 0.75$. Secondly, the identifications for a sample of sources with $S_{408} > 10$ Jy are now almost complete, largely due to prolonged attempts to identify 3CR sources to very faint optical limits.

The technique requires (1) a source count and (2) a luminosity distribution.

3.1 THE SOURCE COUNT AT 408 MHz

The composite differential source count used here is shown in Table 1 and Fig. 2. It has been derived from the following three catalogues:

(1) *The all-sky catalogue of Robertson (1973).* This catalogue, compiled from several surveys, lists all sources stronger than 10 Jy at 408 MHz in all regions of sky away from the galactic plane ($|b| > 10°$, 10.1 sr). It is the best available catalogue of bright sources at this frequency, although it has drawbacks: in particular, most of the flux densities for northern sources were derived by interpolation from other frequencies, and, because parts of the northern finding survey were made with interferometers, some large-diameter sources may be missing. However, these deficiencies are undoubtedly masked by statistical uncertainties in the counts above 10 Jy imposed by the limited total number of sources (160).

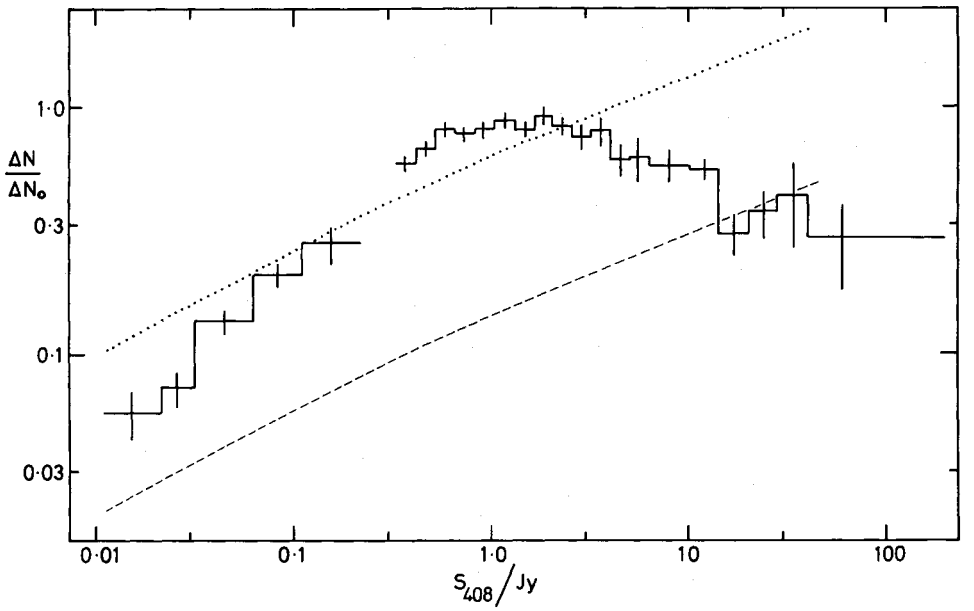

Figure 2. The 408-MHz source count of Table 1, plotted in relative differential form; $N_0 = 1200\,S^{-1.5}$, and error bars correspond to $\sqrt{\Delta N}$. The dashed line corresponds to a source count calculated from the 408-MHz luminosity distribution assuming *no evolution* ($F(P, z) = 1$), and using the technique described in Section 2 with a Friedmann universe, $\Omega = 1$. This technique normalizes the computed count to yield the observed (integral) source surface density at $S_{408} = 10$ Jy, the level at which the luminosity function was constructed. Change of this normalization to yield a best fit by minimizing χ^2 results in the dotted line.

(2) *The Bologna B2 survey (Colla* et al. *1970, 1972, 1973).* The B2 survey covers 1.5 sr to limiting flux densities S_{408} of either 0.20 or 0.25 Jy. The source count from parts 1 to 3 of the survey (9000 sources) is presented by Colla *et al.* (1973). We adopted this count, increasing the flux densities by 6 per cent to correct to the scale adopted in Robertson's catalogue.

Several other 408-MHz surveys have been made covering this flux-density range, notably the One-Mile Telescope fan-beam surveys of Bailey & Pooley (1968) and Willson (1972), which included about 500 sources, and the Molonglo surveys (Davies, Little & Mills 1973; Sutton *et al.* 1974; Robertson 1977a,b) which included about 5000 sources above 0.2 Jy. The published counts from these surveys agree well with those of B2, but to include them in the composite count would not reduce the statistical uncertainty substantially.

(3) *The 5C surveys.* The counts of Fig. 2 were extended down to 10 mJy using the source counts from the 5C2 (Pooley & Kenderdine 1968) and the 5C5 (Pearson 1975) surveys, a total of 304 sources in about 0.004 sr. Surveys 5C1, 3 and 4 are in atypical regions of sky; surveys 5C6, 7 and 9 (Waggett 1977; Pearson & Kus 1978) were incomplete when this compilation was made. The numbers from these latter surveys agree with those of 5C2 + 5C5, and including them would have decreased statistical uncertainties by a factor of about 1.6. Future analyses should incorporate these data, as well as the results of the deep Molonglo surveys (Robertson 1977a, b) which cover the range $S_{408} \geqslant 100$ mJy.

3.2 THE LUMINOSITY DISTRIBUTION AT 408 MHz

To derive a luminosity distribution from a sample of sources complete to a given flux-density limit S_0, each of the sources must be identified optically in order to estimate its distance, ideally from a measured redshift, or at worst from a measured magnitude via a Hubble relation. At present the only completely identified samples are for very large S_0, and

are too small to provide statistically sound luminosity distributions, but a reasonable compromise is possible by adopting a lower value of S_0 and admitting a few unidentified sources whose distances can be guessed.

The sample used here is defined by the criteria:

$S_{408} \geqslant 10\,\mathrm{Jy}$,

$\delta \geqslant -7°$,

$|b| \geqslant 10°$.

The area is 5.86 sr, and the sample is a subsample both of 3CR and of Robertson's catalogue. It contains 87 sources of which 62 (71 per cent) have measured redshifts. The remaining 25 sources are as follows:

Sixteen are identified with galaxies; redshifts for these were estimated from the redshift–magnitude diagram of the other galaxy identifications in the 3CR catalogue.

Two are suggested QSOs; they were arbitrarily assigned $z = 1$ and $z = 2$ respectively.

Seven were not identified. They were assigned redshifts in the range 0.5 to 0.72 consistent with the assumption that the optical counterparts are galaxies fainter than the limiting magnitude of the Palomar Survey prints; there are good arguments for this assumption (e.g. Bolton 1966). This procedure is justified by the most recent optical identification surveys (Gunn *et al.* 1981) in which it has proved possible to identify essentially all the previously unidentified 3CR radio sources in a subset of the statistical sample of 166 sources

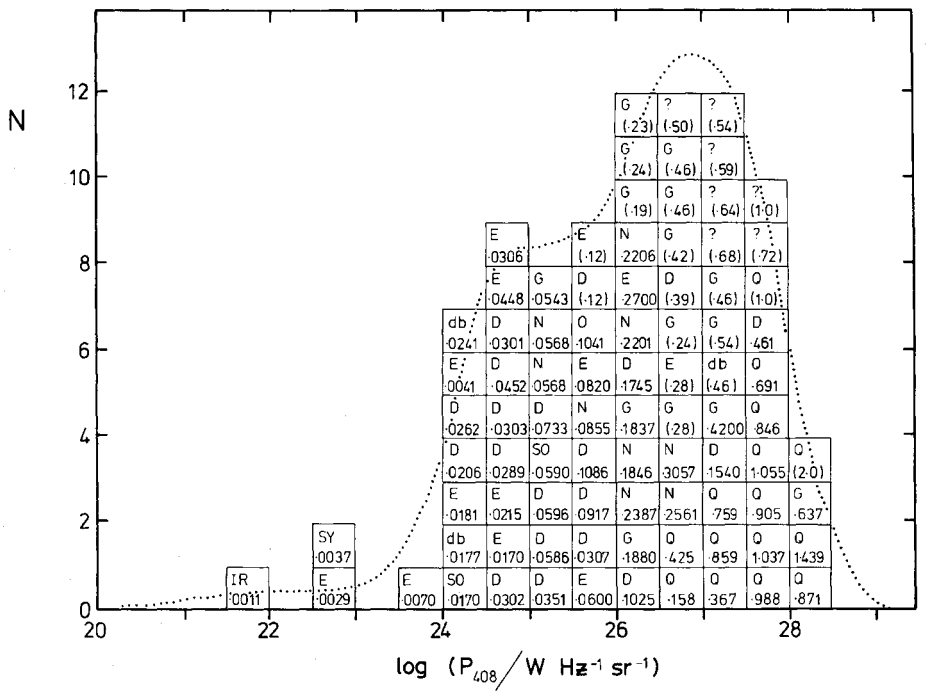

Figure 3. The 408-MHz luminosity distribution ($\Omega = 1$). The sample of 87 sources is complete over 5.86 sr for $S_{408} \geqslant 10$ Jy. The symbols indicating optical counterparts are: Q, QSO; E, N, S0, galaxies of corresponding morphological type; SY, Seyfert galaxy; db, double galaxy; IR, irregular galaxy; G, galaxy of indeterminate type. Unidentified radio sources are indicated as ?. The redshifts in brackets are estimated from apparent magnitudes via a Hubble relation in the case of a galaxy identifications, and for the unidentified sources by assuming that they are galaxies of magnitude just below plate limits. The dotted curve represent the adopted 'master' luminosity distribution, derived by smoothing the unbinned data as described in Section 3. Data from surveys of bright galaxies were used to define the curve at the low-power end.

(Jenkins, Pooley & Riley 1977) by using a CCD detector at the prime focus of the Hale 5-m telescope. Most of these new identifications are with faint galaxies.

In fact, the luminosity estimates are rather insensitive to the estimated redshifts; changing z from 0.5 to 1.0 typically changes P_{408} by a factor of < 5, small in comparison with the total width and main features of the luminosity distribution.

Fig. 3 shows that the sample provides a well-defined luminosity distribution for $P_{408} > 10^{24}\,\mathrm{W\,Hz^{-1}\,sr^{-1}}$, but only four sources of the 87-sample have lower powers. To define this region of the distribution, we have used observations of complete samples of 'normal' galaxies by Caswell & Wills (1967) and Cameron (1971). The luminosity distributions obtained in these investigations were modified (i) by changing the luminosities to conform to $H_0 = 50\,\mathrm{km\,s^{-1}\,Mpc^{-1}}$, and (ii) by changing the numbers in each power bin to correspond to our higher value of $S_0 = 10$ Jy at 408 MHz. For the latter modification, the assumption of uniform spatial distribution was necessary; this is a perfectly safe assumption because the redshifts involved are generally less than 0.1. In the region of overlap between the 'low-power' end of the distribution constructed in this manner and the 'high-power' end defined by the 87-sample, agreement was excellent.

Finally, we convolved all the *unbinned* luminosities of the sources with a Gaussian curve of unit area and $\sigma = 0.4$, and added all the resultant contributions together to produce a smoothed 'master' luminosity distribution for use in the calculations. The value of 0.4 was chosen subjectively; more smoothing smeared real features of the distribution, while less smoothing did not remove enough of the statistical noise. The smooth curve of Fig. 3 is the master luminosity distribution for the $\Omega = 1$ geometry, and a similar curve was obtained for the $\Omega = 0$ geometry.

4 Analysis of the 408-MHz source count; evolution models

4.1 UNSATISFACTORY EVOLUTION MODELS

As a first application of our scheme at 408 MHz, we examined the uniform or non-evolving model. We then examined two models in which the evolution function is represented (for some power range) by analytic functions, namely $(1+z)^{\beta}$ or 'power-law' evolution, and $\exp[M(t_0-t)/t_0]$ or 'exponential' evolution (t is cosmic epoch, t_0 is the present epoch; $t_0 - t$ is often referred to as the 'look-back time'). Both such models were discussed by Doroshkevich, Longair & Zeldovich (1970, hereafter DLZ) to reproduce the 408-MHz count. Exponential models were also discussed by Rowan-Robinson (1970).

4.1.1 The non-evolving model (model 1)

$F(P, z) = 1$; there are no parameters. The count, computed as described in Section 2, is shown in Fig. 2 ($\Omega = 1$). Comparison with observed count yields $\chi^2 = 9732$ for 23 degrees of freedom, indicating that there is one chance in 10^{960} that the differences between model and observation could have arisen by chance. The computational scheme results in a vertical normalization for which the (integral) sky surface densities are forced to agree at 10 Jy. The abandonment of this and optimization of the fit via a vertical re-scaling (see dotted line in Fig. 2) resulted in $\chi^2_{\mathrm{min}} = 545$, again rejecting the non-evolving model but at the lower confidence level of one chance in 10^{80}. Moreover, abandoning the redshift as a distance indicator is of little help: computation of counts for uniformly-distributed source populations of lower luminosities than indicated by the distribution of Fig. 3 results in a set of monotonically-decreasing curves lying between the dashed curve in Fig. 2 and a horizontal line, $\Delta N/\Delta N_0 =$ const. None of these, nor their addition in any proportion, resembles the observed count.

4.1.2 Evolving models

The models of DLZ can be regarded as simple density-evolution models, because the evolution is confined to the powerful sources, and the transition between evolving and non-evolving components is not a function of redshift. DLZ made this transition a gradual one with the following evolution function:

$$F(P, z) = X_1(P) + \phi(z)\, X_2(P), \tag{13}$$

where

$$X_1 = (P_t/P)^n/[1 + (P_t/P)^n]$$

$$X_2 = 1/[1 + (P_t/P)^n]$$

and P_t is the 'transition' power.

(a) 'Power-law' models (model 2)

Here

$$\phi(z) = (1+z)^\beta, z \leqslant z_c \tag{14}$$

and

$$F = 0, z > z_c.$$

Such models were used by Longair (1966), and were subsequently adopted in V/V_{max} analyses (Schmidt 1968). The comoving source density ($P > P_t$) is proportional to power of the scale factor $R(t) = (1+z)^{-1}$ back to a redshift of z_c; at larger redshifts, the density is zero. The cut-off redshift thus corresponds to the epoch of creation of powerful radio sources, the number created at that epoch exceeding the present-day numbers by $(1+z_c)^\beta$, while the number of weak sources ($P < P_t$) created has remained substantially constant. The undetermined parameters are n, P_t, β, and z_c and the ranges of exploration of these are shown in Table 2. Some of these ranges are constrained by observational data. Clearly $z_c < 2$ is inadmissible, and likewise $\log P_t$ must be less than 27.5 (see Fig. 3) in order to permit the strong evolution which Schmidt (1968) found for all QSOs in his subset of 3CR QSOs. The optimum values are also given in Table 2, and the corresponding source-count model in Fig. 4. This count is seen to resemble the observations *qualitatively,* but to be a poor fit

Table 2. Parameter space, 'unsuccessful' models.

Model	Type		Parameters					Chi-square Test	
			M	β	$\log P_t$	z_c	n	χ^2	ν
1	Uniform distribution		–	–	–	–	–	545	22
2	Power law	min	–	5.5	26.5	2.0	0.75		
		max	–	7.0	27.5	4.0	∞		
		~ optimum	–	5.75	27.0	3.0	1.25	151	19
3a	Exponential, no redshift cut-off	min	7.0	–	26.0	–	1.0		
		max	13.5	–	28.0	–	10.0		
		~ optimum	13.5	–	27.3	–	10.0	70	20
3b	Exponential with redshift cut-off	min	7.0	–	25.5	2.0	0.9		
		max	11.5	–	27.5	4.0	2.0		
		~ optimum	10.5	–	27.5	2.0	1.1	87	19

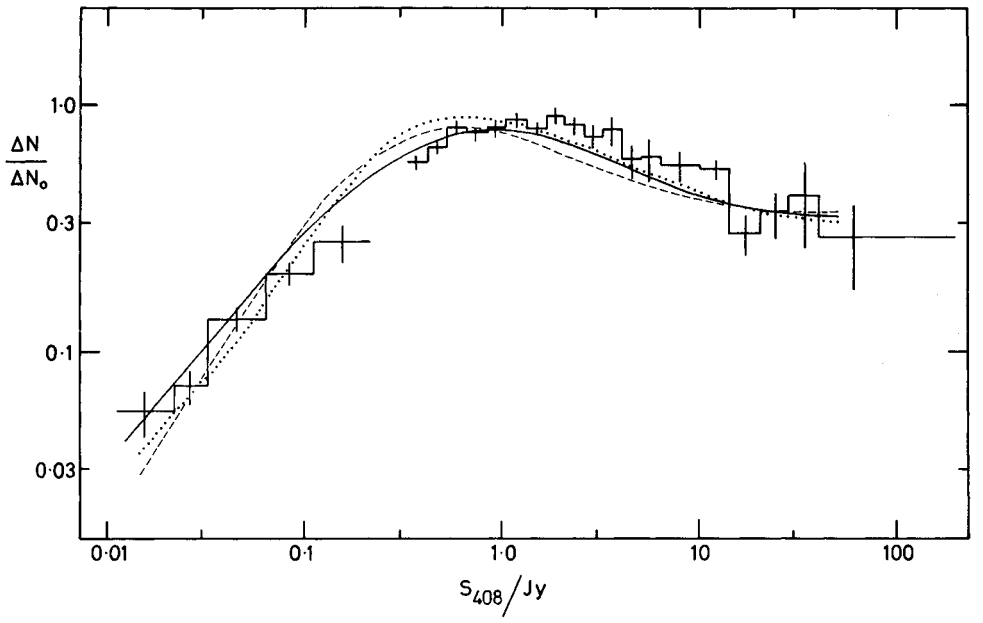

Figure 4. The 408-MHz source count (see caption, Fig. 2), together with best-fitting versions of computed source counts for unsuccessful models of evolution (Section 4.1); parameters for optimum versions of these models are in Table 2. Dashed curve: model 2, 'power-law' with redshift cut-off; solid curve: model 3a, 'exponential' with no redshift cut-off; dotted curve: model 3b, 'exponential' with redshift cut-off.

quantitatively; in fact $\chi^2_{\min} = 151$ (19 degrees of freedom), and the probability of the model accounting for the data by chance is 1 in 10^{10}. The problem is that exponents of $\beta \geqslant 6$ are needed to produce the steep initial rise, while to obtain the observed turnover, values of $z_c < 2.5$ and $\log P_t \geqslant 27.5$ are required. Even when the turnover is achieved using such extreme values, the decrease to the faint flux densities is too rapid. Finally we note that $V/V_{\max}$ data suggest evolution models for which the density increase is higher at small redshifts than for 'power-law' models (Lynds & Wills 1972; Wills & Lynds 1978). This, together with our evidence from the source-count calculations, strongly suggests that 'power-law' models are a poor representation of the cosmological evolution of powerful radio sources.

(b) 'Exponential' models (model 3)

For these

$$\begin{aligned}\phi(z) &= \exp\,[M(1-t/t_0)] \\ &= \exp\,[M(1-(1+z)^{-1}] \text{ for } \Omega = 0 \\ &= \exp\,[M(1-(1+z)^{-3/2})] \text{ for } \Omega = 1,\end{aligned} \tag{15}$$

where t is the epoch corresponding to z, and t_0 is the present age of the Universe. DLZ discussed exponential models because a redshift cut-off is not *a priori* necessary; we investigated models both with and without z_c. The latter model is attractive from a numerical point of view since there are only three parameters, P_t, M, and n. The ranges investigated are shown in Table 2. Best results were obtained for very sharp transitions ($n > 2$) between evolving and non-evolving components. Fig. 5 shows contours of χ^2 as a function of M and P_t with $n = 10$; the minimum (to which the optimum values in Table 2 correspond) is very

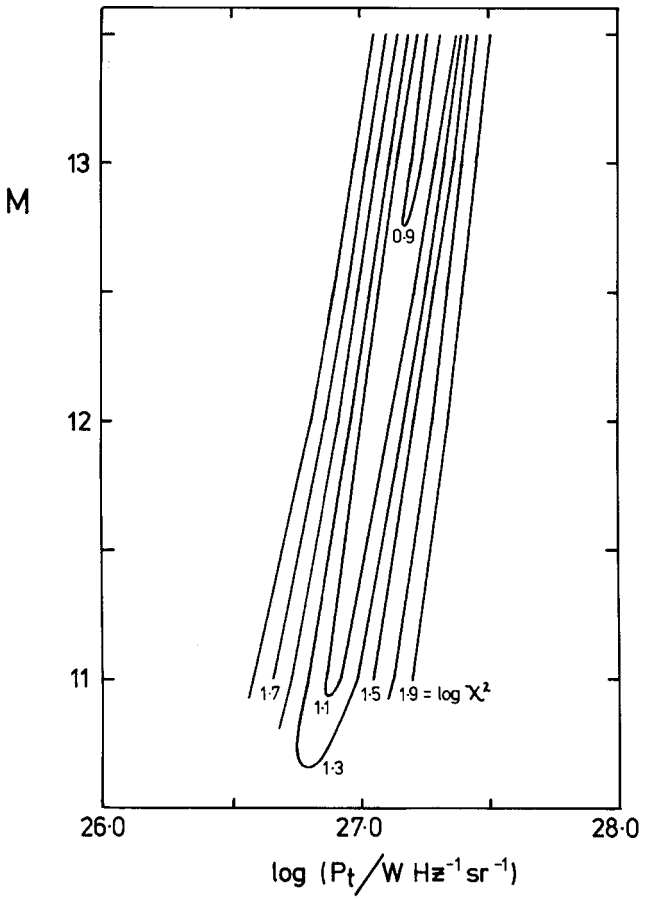

Figure 5. Contours of log (χ^2), the goodness-of-fit parameter, in the M – log P_t plane for unsuccessful model 3a (Table 2). This is the 'exponential' evolution model without redshift cut-off; there are only three parameters, the exponent M, the transition power P_t which divides the strong sources which undergo evolution from the weaker sources which do not evolve, and n, the parameter which describes the sharpness of this transition (equation 12). Here, $n = 10$, and the transition is very abrupt.

sharp, and it is apparent that a slightly improved fit could result from yet higher values of n, M, and P_t. However, the optimum values in Table 2 are upper limits: again, log P_t cannot exceed 27 without excluding a significant proportion of QSOs, while M cannot exceed 13 without producing values of $\langle V/V_{max} \rangle$ well in excess of the observed values of ~ 0.70. The optimum fit is shown in Fig. 4; $\chi^2_{min} = 70$, rejecting the model at the 99.9 per cent level of confidence. The problem is similar to that of the power-law model (but less extreme): it is not possible to satisfy both the steep initial rise and rapid turnover of the count with its steady decline to the fainter flux densities. But there are two other features of this exponential model in which it is difficult to have faith, namely (i) the extreme nature of the transition between evolving and non-evolving sources, and (ii) the fact that the model depends for its 'success' on very significant contributions to the numbers in the lowest flux-density bins from powerful sources at redshifts of 15 to 25.

When a cut-off in redshift is added as a fourth parameter, these very high redshifts in the faint flux-density bins disappear, but the optimum fit becomes even less satisfactory, with $\chi^2_{min} = 87$ for 19 degrees of freedom. The parameter limits and optimum values again appear in Table 2, and the corresponding count in Fig. 4. Replacing an abrupt cutoff at z_c by a gradual cut-off only improves the fit to the extent that the model with redshift cut-off more closely resembles the model without a redshift cut-off.

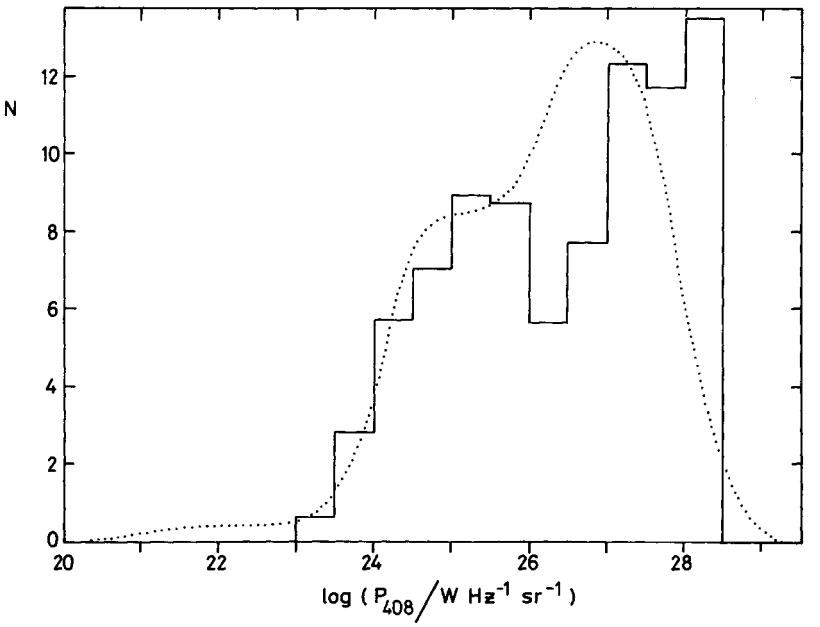

Figure 6. A comparison of the 'master' luminosity distribution (dotted curve; see Fig. 3) with the luminosity distribution (histogram; $S_{408} \geqslant 10$ Jy) implied by the 'power-law' evolution model derived by Doroshkevich *et al.* (1970).

(c) Why did these models fail?

Far from setting statistical limits on the parameters of the models, we conclude that the models themsleves are unsatisfactory. Paradoxically this is encouraging; it suggests that the current data can provide useful constraints on the evolution, and that some *ad hoc* models can be rejected. It is important to know whether the failure of the above models is due to improved data or to the different method of analysis. For this reason, we re-examined model (1) of DLZ (power-law, $\beta = 6$, $\log P_t = 25.50$, $n = 1.5$, $z_c = 3.0$), and the luminosity distribution corresponding to this model (for $\Omega = 1$, $S_{408} = 10$ Jy) is shown in Fig. 6. Although it is incompatible with the luminosity distribution of Fig. 3 which forms the basis for the present analysis, the difference is hardly large enough to lead to the rejection of the model now, and indeed a simpler answer emerged from re-computing the count itself – a χ^2-test against the observed count yielded $\chi^2_{\min} = 107$ (20 degrees of freedom), indicating that the model did not provide a satisfactory source count *ab initio* (although, of course, the DLZ 408-MHz source counts were defined with poorer statistical precision than those of Fig. 2). DLZ emphasized that their aim was to examine *qualitative* requirements of the evolution function; our analysis confirms their qualitative conclusions, but demonstrates that the models are *quantitatively* unsatisfactory. It is also salutary to note that the apparent agreement of the DLZ models came about by comparison with an *integral* form of the source count. The dangers of using integral counts have been emphasized by Jauncey (1967).

4.2 SATISFACTORY EVOLUTION MODELS

Two models satisfying the data of Section 3.1 were obtained from very different approaches.

(a) *An exponential model with $M = M(P)$ (model 4).* The first of these approaches was to consider the $V/V_{\max}$ statistic for the complete sample of 3CR sources (Jenkins *et al.* 1977). For this sample (essentially complete for $S_{408} > 5$ Jy), values of $V/V_{\max}$ were calculated using the radio limit only, a and a plot was constructed of $\langle V/V_{\max} \rangle$ against $\log P_{408}$. For a

given world model, there is a one-to-one relation between the value of $\langle V/V_{max} \rangle$ and M, the exponent in the exponential evolution function. The plot suggested that a satisfactory form of the evolution function might be one in which the parameter M in the exponential model (equation 14) is a function of P_{408} of the following form:

$M(P) = 0$ for $P < P_1$,

$M(P) = M_{max}$ for $P > P_2$,

and

$$M(P) = M_{max}\ (\log P - \log P_2)/(\log P_2 - \log P_1), \tag{16}$$

where

$F(P, z) = \exp\ [M(P)\ (1 - t/t_0)]$.

The transition between evolving and non-evolving components is very different from that of the previous exponential model, and it is this different transition which leads to the relative success. This success is not total, in that parameter searches failed to find a satisfactory fit for the $\Omega = 0$ geometry. The count calculated in this geometry shows the objectionable

Table 3. Parameters, 'successful' models ($\Omega = 1$).

Model	Type	~ Optimum parameters	Chi-square Test χ^2	ν
4a	Exponential, $M = M(P)$ No redshift cut-off	$\log P_1 = 26.0$, $\log P_2 = 27.1$, $M_{max} = 11.5$.	31.7	20
4b	As for 4a, but with redshift cut-off	$\log P_1 = 25.0$, $\log P_2 = 27.3$, $M_{max} = 11.0$, $z_c = 3.5$.	29.6	19
5	As for 3a, but with log $P_t = a \log z + b$	$M = 9.8$, $a = 3.14$, $b = 26.8$, $n = 1.06$	23.8	19

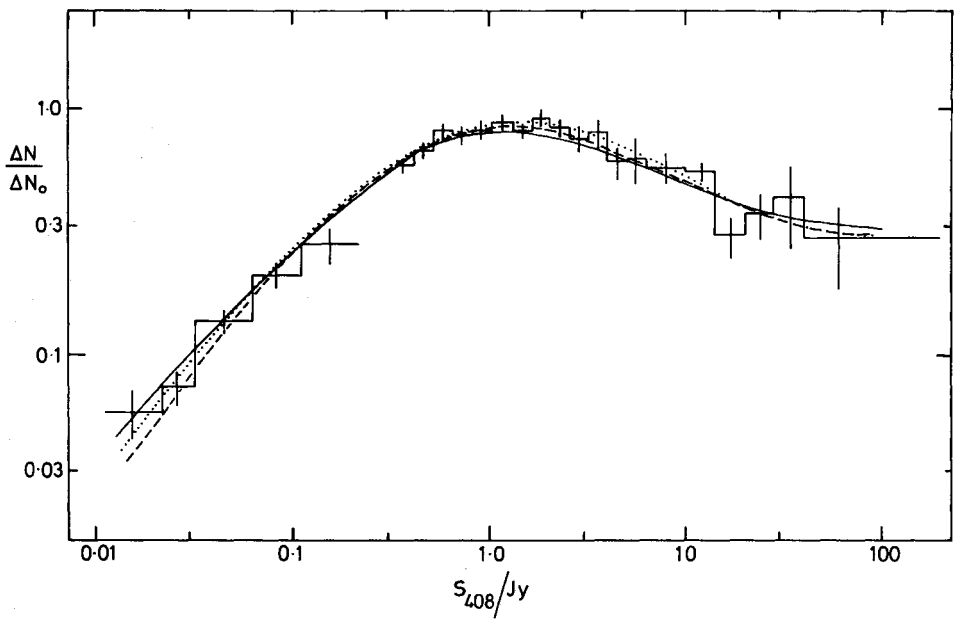

Figure 7. The 408-MHz source count (see caption, Fig. 2), together with source counts computed for the successful evolution models of Section 4.2. Solid curve: model 4a ('exponential', no redshift cut-off); dashed curve: model 4b ('exponential' with redshift cut-off); dotted curve: model 5 ('exponential' with $P_t = P_t(z)$). Parameters are given in Table 3.

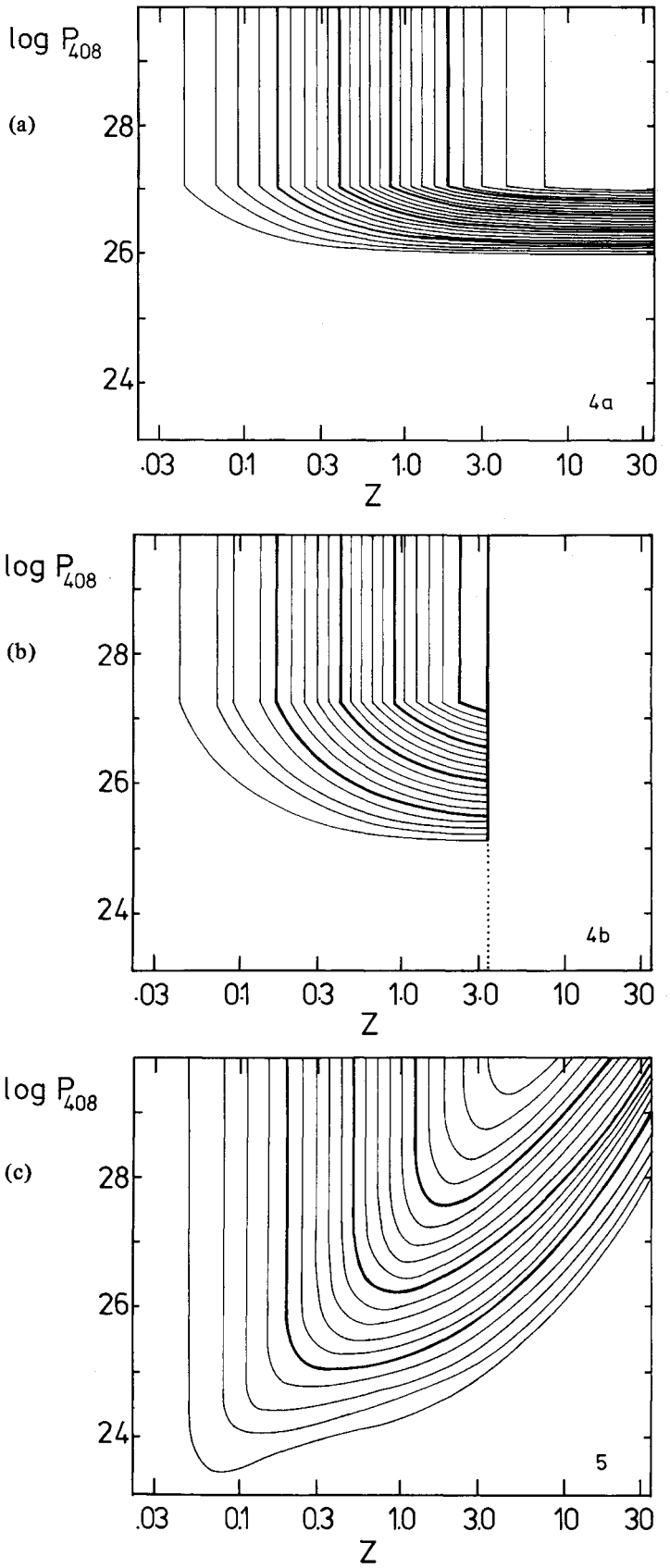

Figure 8. Contours of density enhancement $F(P, z)$ in the evolution plane for the successful evolution models 4a, 4b and 5 derived in Section 4. Parameters are given in Table 3. The heavy contours represent log F = 1, 2, 3, 4, and the light contours log F = 0.2, 0.4, 0.6 etc. The dotted line represents the redshift cut-off (model 4b), to the right of which $F(P, z) = 0$.

Table 4. Identification content, 408-MHz samples.

(1)	B2 (Grueff & Vigotti 1977)	
	526 Sources, $m_R \leqslant 20.5$, $S_{408} \geqslant 0.9$ Jy	
	Galaxies	40 per cent
	Unconfirmed QSOs	23 per cent
	Empty fields	37 per cent
		100 per cent
(2)	5C6/5C7 (Perryman 1979a, b)	
	563 Sources, $V \leqslant 22$, $S_{408} \geqslant 10$ mJy	
	Galaxies	8 per cent
	Unclassified objects	9 per cent
	Unconfirmed QSOs	4 per cent
	Empty fields	79 per cent
		100 per cent

features of the counts from previous exponential models; but in the $\Omega = 1$ universe, the relatively small (comoving) volume elements for given Δz's assist in producing the gradual decrease in the counts as observed. Optimum parameters for this universe are given in Table 3, and the source count is shown in Fig. 7. A redshift cut-off z_c can be imposed as a fourth parameter, and Table 4 gives the optimum parameter set for this version of the model (model 4b); again no satisfactory set could be found for the $\Omega = 0$ geometry. Contours of density enhancement in the P–z 'evolution' plane are shown in Fig. 8.

A feature of interest with regard to this model is that a successful evolution model to describe the source count down to the faintest levels observed could be derived by considering the spatial distribution of the bright sources alone. The model emphasizes the complementary nature of V/V_{max} and count data in such studies.

(b) *An exponential model with $P_t = P_t(z)$ (model 5).* A second successful model produced a significantly better fit to the counts, and encountered no difficulties in the $\Omega = 0$ geometry. It was derived by inspection of the population of the S–z plane for unsuccessful models, from which it was evident that the desired behaviour of the source count could be achieved by narrowing at the larger redshifts the range of power for which evolution applies. To do so, we retained the formulation of the unsuccessful exponential model (equation 15), but rather than put P_t = constant, we use

$$\log P_t = a \log z + b. \tag{17}$$

Optimum values for the four parameters of the model are given in Table 3; the relatively small value of χ^2_{min} indicates the success of the model. The narrowing of the range of evolving powers at large redshifts results in a smooth decrease in the counts to the fainter flux densities, as required. Moreover, evolution is not ruled out for all sources with log $P_{408} < 10^{27}$, and in particular, the predicted $\langle V/V_{max} \rangle$ results for different powers agree with the observations to within statistical uncertainty. Contours of $F(P, z)$ are shown in Fig. 8.

4.3 SCRUTINY OF THE 'SUCCESSFUL' MODELS

4.3.1 The local luminosity function

Our technique produces *local* ($z = 0$) *luminosity functions* ($\rho(P, z = 0) = \rho_0$) as by-products of the calculations via equation (9). This function is different for each assumed evolution

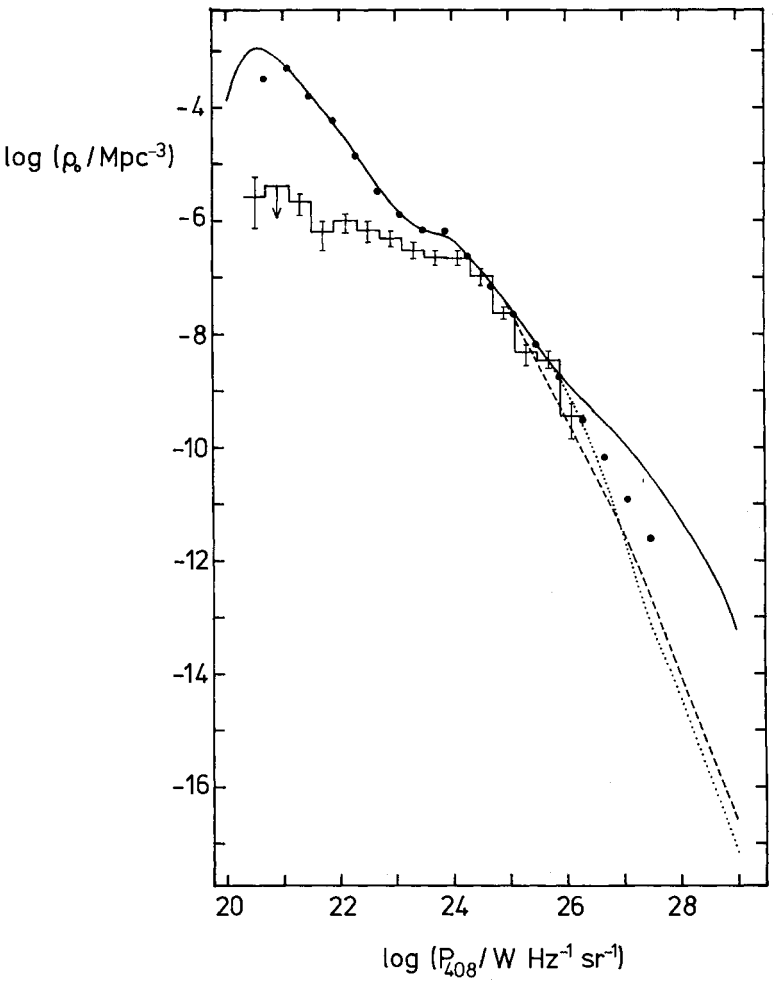

Figure 9. The local luminosity function. The curves represent ρ_0 as derived in the present calculations via equation (9). The solid curve results from unsuccessful model 1 (no evolution). The dotted curve results from successful models 4a and 4b (parameters are in Table 3) while the dashed curve results from model 5; at the lower powers, these curves are identical with the 'no evolution' curve. The heavy dots represent Longair's (1971) tabulated luminosity function, and the steps show the luminosity function for elliptical galaxies obtained by Auriemma *et al.* (1977). Both of these have been scaled to $H_0 = 50\,\mathrm{km\,s^{-1}\,Mpc^{-1}}$, and to 408 MHz via $\alpha = 0.75$.

model, and local luminosity functions for successful evolution models are shown in Fig. 9 to illustrate this point. The solid curve represents the local luminosity function in the absence of evolution, i.e. for the unsuccessful model 1. For a given *luminosity distribution,* as assumed in our procedure, evolution must depress the local luminosity function below the 'no-evolution' function; see equation (9). In Fig. 9, the dotted curve results from successful models 4a and 4b (the individual curves for these being indistinguishable), while successful model 5 yields the dashed curve. The evolution extends to lower powers for model 5 than for model 4, which explains the differences in the two curves. At powers below 10^{24} $\mathrm{W\,Hz^{-1}\,sr^{-1}}$, all three curves are identical because none of the models ascribes evolution to weak sources.

It is of interest to compare the present estimate of $\rho_0(P)$ with that of Longair (1971); Longair's tabulation is for 178 MHz and $H_0 = 75\,\mathrm{km\,s^{-1}\,Mpc^{-1}}$. The heavy points in Fig. 9 show his tabulation transformed to 408 MHz using $\alpha = 0.75$, and to $H_0 = 50\,\mathrm{km\,s^{-1}\,Mpc^{-1}}$. Agreement at $P_{408} < 10^{25}\,\mathrm{W\,Hz^{-1}\,sr^{-1}}$ is excellent, a result which is not surprising because the same bright sources in the northern sky were used in both derivations. At $P_{408} > 10^{25}$

$W\,Hz^{-1}\,sr^{-1}$ Longair's ρ_0 lies above the best estimates from the present work. The reason is evident from Fig. 6. The *luminosity distribution* implicit in the earlier work (e.g. DLZ) is at odds with modern data in that it contains too many sources at high luminosities. In addition, the figures quoted in the 1971 paper were derived on the basis of power-law evolution which gives too little evolution at small redshifts. However, the 'successful' evolution models from these analyses and from the present analysis are quantitatively similar, although differing somewhat in detail. The ρ_0 obtained in the earlier work must therefore produce space densities at the higher powers which are significantly greater than those from the present work.

Auriemma *et al.* (1977) estimated the local bivariate luminosity function for elliptical galaxies by combining V/V_{max} results for four complete samples. The local radio luminosity function which they derived (obtained by summing the bivariate luminosity function across all optical luminosities $M<-18$) is shown by the histogram in Fig. 9. Auriemma *et al.* compared their result with a preliminary version of the present local luminosity function, and correctly concluded that the divergence below $\log P_{408} = 24$ is due in the main to *spiral* galaxies; our determination comprises all types of galaxy. At $\log P_{408} > 24$, the Auriemma *et al.* determination is in good agreement with ours, close enough for the differences to be statistical only. This value of radio luminosity is of some interest; the contribution of spiral galaxies has completely disappeared, and the radio structures are no longer confined to the optical disc, but take on the well-known double-lobe appearance. The intersection at $\log P_{408} \simeq 24.5$ therefore provides a natural division between 'normal' and 'radio' galaxies.

4.3.2 Behaviour of the luminosity function

It is clear from Fig. 8 that the two 'successful' models ascribe very different cosmic histories to the 'steep-spectrum' radio-source population. These differences are reflected in the variation of the predicted redshift distributions with flux density shown in Fig. 10; the differences in the S–z plane naturally are maximized at the faintest flux-density level for which the counts are calculated. The differences are so large as to suggest that constraints can be placed on the evolution function from *identification content* of complete samples of faint sources, without the necessity of obtaining redshifts for each of the objects.

As an illustration, we compare the predictions of the models with two samples, one from the B2 catalogue (Grueff & Vigotti 1977) and the other from the 5C6 and 5C7 surveys (Perryman 1979a, b). The specifications and identification contents of the samples are given in Table 4. With regard to the B2 sample, Grueff & Vigotti claim that the identifications are complete to $m_R = 20.5$. An extrapolation of the relevant $m_R - z$ (Hubble) relation (their Fig. 4) suggests that this corresponds to $z = 0.75$ for galaxy identifications. If the redshift distribution of B2 QSO identifications is the same as that compiled for known radio QSOs by Ricklefs & Wills (1976), then 35 per cent have $z < 0.75$. The total proportion of identifications with $z < 0.75$ is then about (40 per cent (galaxies) + 0.35 x 23 per cent (QSOs)) = 48 per cent. For the 5C6/5C7 sample, Perryman (1979a, b) adopted a limiting magnitude of $V = 22$ for the plates obtained by M. V. Penston with the 48-inch Hale Schmidt telescope which were used in the investigation. Extrapolation of the Hubble relation for 3CR galaxy identifications (Section 3) suggests a limiting redshift for galaxy identifications of 0.6. On the further assumptions (i) that the unclassified identifications near the plate limit are galaxies, and (ii) that as for B2, the QSO identifications follow the redshift distribution given by Ricklefs & Wills, the total proportion of sources in the sample with $z < 0.6$ is about 18 per cent.

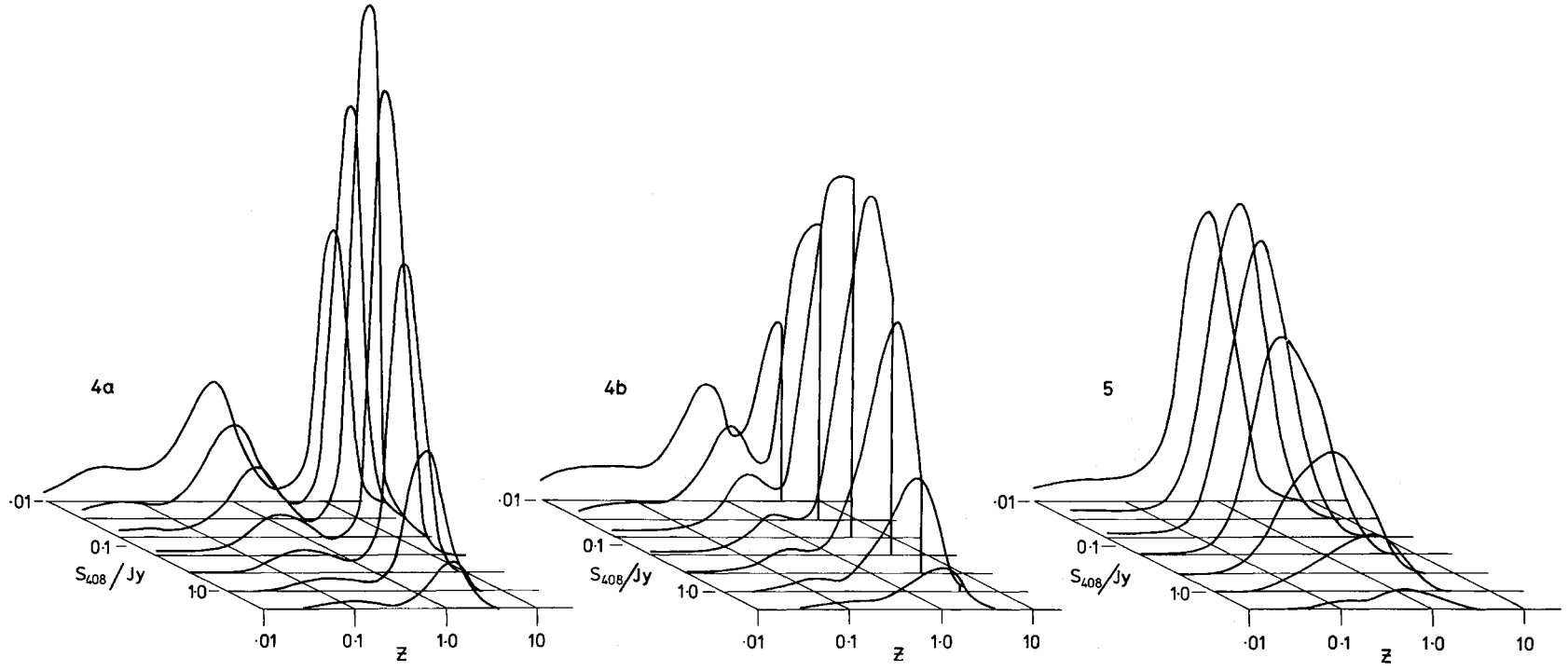

Figure 10. The distribution of redshifts for radio sources, $N(z)$, as a function of flux density predicted by successful evolution models 4a, 4b and 5 (parameters in Table 3). For models 4a and b, the distribution $N(z)$ becomes double-peaked as flux density decreases, and for model 4a, the curves at $S_{408} < 0.3$ Jy show substantial numbers of sources at $z > 10$. Model 4b has a redshift cut-off at $z = 3.5$, resulting in a greater proportion of sources occurring at lower redshifts amongst the fainter flux bins than for model 4a; the identification proportion at low flux levels is consequently predicted to be higher (Table 6). Model 5, which incorporates some luminosity evolution, yields distributions with a single maximum, the maximum occurring near $z = 1$ for all flux-density levels.

Table 5. Predicted redshift proportions.

	Fraction with	Model 4a (per cent)	Model 4b (per cent)	Model 5 (per cent)	Observed (per cent)
(B2)	$z < 0.75, S_{408} \geqslant 0.9$ Jy	28.4	40.2	75.3	48
(5C)	$z < 0.6\ S_{408} \geqslant 10$ mJy	26.1	32.3	47.9	18

The comparisons with models 4a, 4b and 5 appear in Table 5. For each of the two samples, model 5 predicts too large a proportion of identifications, these large proportions coming about via the evolution which the model ascribes to source of relatively low luminosity as shown in Fig. 8. Model 4b is favoured by the B2 sample and model 4A by the 5C sample, but the very large uncertainties in the samples – magnitude estimates, completeness limits, extrapolated Hubble relations, QSO redshift distributions – do not permit definitive conclusions. Nevertheless the analysis does show that compilations at fainter flux-density levels of identification samples with accurate magnitudes are crucial in constraining evolution models. The analysis further suggests that when such samples are completed, models of type 5 are unlikely to survive.

5 Discussion

Two recent investigations have suggested that there has been little evolution at recent epochs. Meier *et al.* (1979) used the maximum-volume method to construct radio luminosity functions from elliptical galaxies identified in three samples of radio sources selected from the 3CR and Bologna B2 catalogues. They considered bright galaxies ($m < 17$), extending out to $z \sim 0.12$ and found that the radio luminosity functions for different redshift ranges within the limiting redshift of 0.12 were identical. Implications for a variety of models are discussed, and in particular it was shown that the popular model in which the 'break' in the luminosity function is caused by death of the high-luminosity sources is not tenable.

Katgert, de Ruiter & van der Laan (1979) attempted identifications for large samples of radio sources found in deep Westerbork surveys (1400 MHz), using deep plates from the 4-m telescope of Kitt Peak National Observatory and from the 48-inch Hale Schmidt telescope. By means of the maximum-volume method, they constructed radio luminosity functions for different ranges in apparent magnitudes, then estimated redshifts from these magnitudes by means of an adopted Hubble relation, and found that all luminosity functions for $z < 0.25$ are similar, with an evident increase in space density for higher redshifts. Katgert *et al.* suggested that this change in space density corresponds to a dramatic change in colour, radio galaxies at $z > 0.4$ appearing some 2 mag bluer on their plates than those at the present epoch. Such an enormous colour change is difficult to understand in terms of the physical evolution of galaxies, and requires confirmation from calibrated plates. However, the absence of evolution at small redshifts is in agreement with the results of Meier *et al.*, and is complementary in demonstrating that radio galaxies with $P_{408} > 10^{25}\,\mathrm{W\,Hz^{-1}\,sr^{-1}}$ at small redshifts also show little cosmological evolution.

Katgert *et al.* emphasized that the absence of evolution at $z < 0.25$ is apparent on the bases of 3CR data alone. It is thus demonstrable with the data tabulated herein, as has been shown by J. Allington-Smith (private communication).

Robertson (1978, 1980) developed an iterative scheme to find optimum 'free-form' evolution for the steep-spectrum sources. His second paper (1980) in fact used the *luminosity distribution* as the starting point as described herein and by WPL. Robertson attempted to define the population of the evolution (P–z) plane without recourse to arbitrary analytical functions such as those adopted here. However, his 'free-form' is in reality a highly restricted form in that he adopted a transition between evolving and non-evolving sources

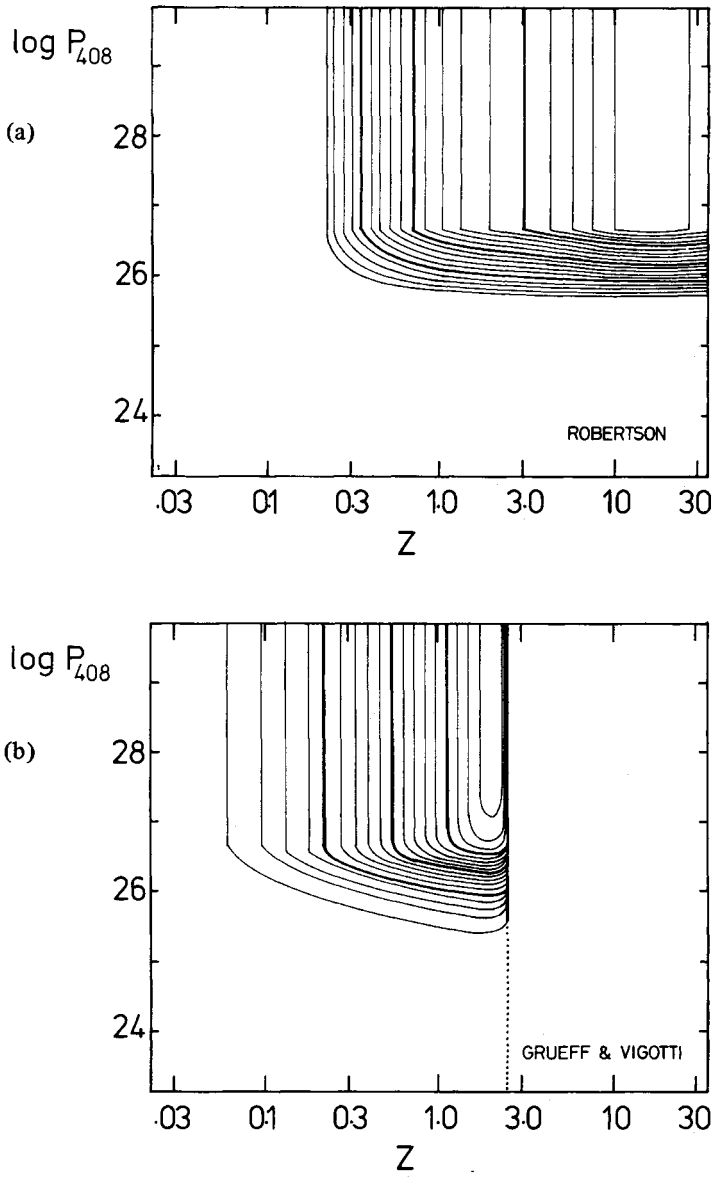

Figure 11. Contours of density enhancement in the P–z evolution plane for (a) Robertson's (1980) numerical evolution model, and (b) Grueff & Vigotti's (1977) 'semi-physical' evolution model. The contours are as described in the caption to Fig. 8.

which is independent of redshift and of a particular parametric form. There is no guarantee that *density evolution,* as such a formulation is usually described, is valid. The density enhancements derived by Robertson (1980) are contoured in Fig. 11. Two points are of interest: (i) the absence of evolution at small redshifts suggested by Meier *et al.*, by Katgert *et al.*, and by Allington-Smith, is evident in Robertson's iterative solution, and (ii) the transition power is very similar to that obtained for models 4a and 4b (Table 4, Fig. 8).

Grueff & Vigotti (1977) proposed a scheme for the evolution of radio sources in which the spatial distribution of QSOs and radio galaxies are causally linked in the following way. All radio sources are born in QSOs at $z = 2.5$, a QSO being regarded as the hyper-active nucleus of a giant elliptical galaxy. The comoving density of QSOs decreases exponentially with epoch, leaving radio galaxies which live for times taken to be inversely proportional to radio luminosity. A model with these assumptions, a guessed radio luminosity function for QSOs at birth ($z = 2.5$), and four parameters, yields remarkably good agreement with

low-frequency source counts and identification data, particularly the proportions of QSOs and radio galaxies as a function of flux density. Differential evolution comes about because the density of radio galaxies decreases with a time-constant depending upon radio power; radio galaxies of low luminosities have time-constants longer than the Hubble time $1/H_0$, resulting in little or no change of density with epoch. The population of the P–z plane produced by the Grueff–Vigotti model is shown in Fig. 11. The resemblance to model 4b (Fig. 8) is striking.

A χ^2-test of the 408-MHz source count produced by the Grueff–Vigotti model against the observed count serves to 'reject' the model, but only at the 2 per cent level of the significance (Grueff, private communication). The fit is thus not unreasonable even though Grueff & Vigotti made no attempt to find the optimum parameter set. Moreover, it is important to emphasize that the goodness-of-fit must be much worse to reject physical (or even semi-physical) models of evolution than to reject the purely numerical models derived in this paper.

The results of the calculations given here represent first steps only. It is particularly encouraging that the constraints imposed are severe enough to reject many of the *ad hoc* evolution models in the literature – and in particular those of the form $(1+z)^{\beta}$. We have presented some new and acceptable models, but we stress that their main role is illustrative, and indicate the level of the complexity now necessary to explain all the observational data. These models show that a large range of populations for the P–z plane is still permitted, and that surveys and identification programmes to faint radio and optical levels can provide powerful further constraints on the evolution of steep-spectrum, extended radio sources.

In Paper II, we apply the technique to source counts and identification data at a higher frequency, in order to derive broad constraints on the spatial distribution of the flat-spectrum, compact radio sources.

Acknowledgments

We thank Peter Warner for help and advice on computing techniques. JVW gratefully acknowledges support of the Royal Society via a Jaffé Donation Research Fellowship held during the course of this work.

References

Auriemma, C., Perola, G. C., Ekers, R., Fanti, R., Lari, C. Jaffe, W. J. & Ulrich, M.-H., 1977. *Astr. Astrophys.*, **57**, 41.

Bailey, J. A. & Pooley, G. G., 1968. *Mon. Not. R. astr. Soc.*, **138**, 51.

Bolton, J. G., 1966. *Nature*, **211**, 917.

Cameron, M. J., 1971. *Mon. Not. R. astr. Soc.*, **152**, 403.

Caswell, J. L. & Wills, D., 1967. *Mon. Not. R. astr. Soc.*, **135**, 231.

Colla, G., Fanti, C., Fanti, R., Ficarra, A., Formiggini, L., Gandolfi, E., Grueff, G., Lari, C., Padrielli, L., Roffi, G., Tomasi, P. & Vigotti, M., 1970. *Astr. Astrophys. Suppl.*, **1**, 281.

Colla, G., Fanti, C., Fanti, R., Ficarra, A., Formiggini, L., Gandolfi, E., Lari, C., Marano, B., Padrielli, L. & Tomasi, P., 1972. *Astr. Astrophys. Suppl.*, **7**, 1.

Colla, G., Fanti, C., Fanti, R., Ficarra, A., Formiggini, L., Gandolfi, E., Gioia, I., Lari, C., Marano, B., Padrielli, L. & Tomasi, P., 1973. *Astr. Astrophys. Suppl.*, **11**, 291.

Davies, I. M., Little, A. G. & Mills, B. Y., 1973. *Aust. J. Phys. Astrophys. Suppl., No. 28.*

Doroshkevich, A. G., Longair, M. S. & Zeldovich, Y. B., 1970. *Mon. Not. R. astr. Soc.*, **147**, 139.

Grueff, G. & Vigotti, M., 1977. *Astr. Astrophy.*, **54**, 475.

Gunn, J. E., Hoessel, J. G., Westphal, J. A., Perryman, M. A. C. & Longair, M. S., 1981. *Mon. Not. R. astr. Soc.*, in press.

Jauncey, D. L., 1967. *Nature*, **216**, 877.

Jauncey, D. L., 1977. *Radio Astronomy and Cosmology, IAU Symp. 74,* D. Reidel, Dordrecht.
Jenkins, C. J., Pooley, G. G. & Riley, J. M., 1977. *Mem. R. astr. Soc.,* **84,** 61.
Katgert, P., de Ruiter, H. R. & van der Laan, H., 1979. *Nature,* **280,** 20.
Longair, M. S., 1966. *Mon. Not. R. astr. Soc.,* **133,** 421.
Longair, M. S., 1971. *Rep. Prog. Phys.,* **34,** 1125.
Longair, M. S., 1978. In *Observational Cosmology,* Eighth Advanced Course of the Swiss Society of Astronomy and Astrophysics p. 125, eds Maeder, A., Martinet, L. & Tammann, G., Geneva Observatory.
Longair, M. S. & Scheuer, P. A. G., 1970. *Mon. Not. R. astr. Soc.,* **151,** 45.
Lynds, C. R. & Wills, D., 1972. *Astrophys. J.,* **172,** 531.
Meier, D. L., Ulrich, M.-H., Fanti, R., Giola, I. & Lari, C., 1979. *Astrophys. J.,* **229,** 25.
Pearson, T. J., 1975. *Mon. Not. R. astr. Soc.,* **171,** 475.
Pearson, T. J. & Kus, A. J., 1978. *Mon. Not. R. astr. Soc.,* **182,** 273.
Perryman, M. A. C., 1979a. *Mon. Not. R. astr. Soc.,* **187,** 223.
Perryman, M. A. C., 1979b. *Mon. Not. R. astr. Soc.,* **187,** 683.
Pooley, G. G. & Kenderdine, S., 1968. *Mon. Not. R. astr. Soc.,* **139,** 529.
Ricklefs, R. L. & Wills, D. 1976. *Mon. Not. R. astr. Soc.,* **175,** 81P.
Robertson, J. G., 1973. *Aust. J. Phys.,* **26,** 403.
Robertson, J. G., 1977a. *Aust. J. Phys.,* **30,** 209.
Robertson, J. G., 1977b. *Aust. J. Phys.,* **30,** 231.
Robertson, J. G., 1978. *Mon. Not. R. astr. Soc.,* **182,** 617.
Robertson, J. G., 1980. *Mon. Not. R. astr. Soc.,* **190,** 143.
Rowan-Robinson, M., 1970. *Mon. Not. R. astr. Soc.,* **150,** 389.
Scheuer, P. A. G., 1975. In *Galaxies and the Universe,* vol. 9, *Stars and Stellar Systems,* p. 725, eds Sandage, A., Sandage, M. & Kristian, J., University of Chicago Press.
Schmidt, M., 1968. *Astrophys. J.,* **151,** 393.
Sutton, J. M., Davies, I. M., Little, A. G. & Murdoch, H. S., 1974. *Aust. J. Phys. Astrophys. Suppl. No. 33.*
Waggett, P. C., 1977. *Mon. Not. R. astr. Soc.,* **181,** 547.
Wall, J. V., Pearson, T. J. & Longair, M. S., 1977. I *Radio Astronomy and Cosmology, IAU Symp. 74,* p. 269, ed. Jauncey, D. L., D. Reidel, Dordrecht.
Wills, D. & Lynds, C. R., 1978. *Astrophys. J., Suppl.,* **36,** 317.
Willson, M. A. G., 1972. *Mon. Not. R. astr. Soc.,* **156,** 7.